

# An Interactive Segmentation Method of LiDAR Data

Wen-Hui Li

College of Computer Science and Technology, Jilin University, Changchun, China

Email: liwh@jlu.edu.cn

Hong-Yin Ni

College of Computer Science and Technology, Jilin University, Changchun, China

Email: nihongyin@163.com

Hui-Ying Li and Ying Wang and Bo Fu and Yi-Feng Lin and Pei-Xun Liu

College of Computer Science and Technology, Jilin University, Changchun, China

Email: {lihuiying@jlu.edu.cn, wangying\_jlu@163.com, fubocloud@163.com, linyifeng\_jlu@yahoo.cn, liupeixun\_jlu@163.com}

**Abstract**—In order to alleviate the problems inherent of automatic segmentation of LiDAR data, an interactive graph-cut segmentation method of LiDAR data is proposed. Firstly, the research background and the basic conceptions of the interactive graph-cut algorithm are introduced. Secondly, by analyzing the characteristics of LiDAR data, four-dimensional feature vectors are extracted, which as the graph-cut algorithm's input. Thirdly, the optimal parameter is estimated according to a new Sample-fitting method. At last, the experimental results show that this interactive segmentation method of LiDAR data is able to accurately locate the buildings region with less interaction, and at the same time guarantee the accuracy rata when buildings and trees are connected to each other.

**Index Terms**—feature extraction, segmentation, graph-cut, sample-fitting, LiDAR

## I. INTRODUCTION

Light Detection and Ranging (LiDAR) is an active remote sensing system developed in the early nineties, which utilizes laser beam to detect and measure the surface information of urban area with high spatial and temporal resolution. As we all know, Laser Radar or Airborne Laser Scanning System (ALSS) [1] is one of the most commonly used system, which can be applied to measure range and reflectance of objects on the earth surface. Using LiDAR for urban area data capturing is an

accurate, fast, high-density and versatile measurement technique. Compared to traditional photogrammetry, LiDAR is low cost and can be more widely applied to extracts the patches of objects at a different height, such as feature extraction[2] and the reconstruction of terrain[3], buildings[4, 5], roads[6] etc.

Building is the main indispensable component to form a city. The more accurate buildings information extracted, the more accurate models reconstructed. Currently, how to get the accurate building information from LiDAR is a popular subject. However, building extraction is an extremely difficult task because of the complex diversity of buildings and other targets' interference, such as vegetations, trees etc.

Many researchers have proposed different methods for building extraction using LiDAR data. Some researchers extract and classify object information in LiDAR data directly. In [5], the author presents an automatic approach to extracts efficient geometric features based on discrete differential geometry theory. Then the outlines of buildings are extracted automatically according to the discrete curvature analysis of all LiDAR points' geometric characteristics. In [7], LiDAR points are rasterizing into Digital Surface Model (DSM). Then the morphological method and alpha Shapes algorithm applied to DSM for extracting buildings. In [8], the author applies a special region growing method to LiDAR data for obtaining objects, such as trees, buildings and terrain objects. Then object specific features are extracted and classified by means of a fuzzy logic approach. However, building extraction is awfully difficult owing to the discrete distribution of LiDAR data and the building's points mingled in the vegetation's points. Some researchers attempt to get objects according to the combination of LiDAR data and corresponding aerial image. In [9], an approach is proposed for building extraction based on LiDAR data and corresponding aerial

Manuscript received January 20, 2012;

Nation Nature Science Foundation: No 60873147; Science and Technology Development Program of Jilin Province: No 20060527

Corresponding Author: Wen-Hui Li (1961 –): Male, Ph D. His major research interests include computer vision, image processing, pattern recognition, graphics, virtual reality, CAD and geometric constraint.

image. Firstly, a gray image can be calculated by height information of the points in LiDAR Data. Then the outlines of objects are extracted from the image and the textures of the objects are obtained from corresponding aerial images. In [10], the author combines LiDAR data with CCD images obtained simultaneously, which is applied to improve the accuracy of object extraction. By the intensity of CCD images, LiDAR data can be classified by its' color and intensity. Then a Building extraction method is presented by integrating the spectral, intensity and spatial attributes of return points. However, there are also some disadvantages in these methods: increasing equipment costs and matching difficulty.

In this paper, according to the current research actuality, the interactive graph-cut method is described and analyzed in detail [11, 12]. Then an undirected graph  $G$  is constructed by LiDAR points as nodes, nodes connected with adjacent nodes as edges. Subsequently, the 4-D feature vectors of LiDAR points cloud are proposed to calculate the boundary energy and regional energy of the undirected graph  $G$ . Finally, optimal binary segmentation is obtained by solving a graph-cut problem.

II. INTERACTIVE GRAPH-CUT THEORY

Interactive graph-cut method [11] has been widely applied to segment image. It is a useful tool to get the minimize energy. The result of this method is that an image is divided into two parts: "object" set and "background" set. In segmentation process, additional constraints for segmentation must be satisfied: certain pixels belong to "object" and certain pixels belong to "background".

In [11], the author considers the constraints of interactive graph-cut method are obtained by computing certain property of segmentation areas. In an image, some pixels were marked as internal pixels and some as external pixels. The border of segmentation can separate the "object" pixels from the "background" pixels. The author verifies the accuracy of graph-cut algorithm.

In this section, some basic conceptions of graph cuts are introduced. Let  $G = \langle V, E, W \rangle$  is a weighted graph with node set  $V$ , edge set  $E$  and weight set  $W$ . All edges in  $G$  are assigned weights like this:  $\{w_e | e \in E\}$ . If a subset  $C \subset E$  satisfies the condition sub-graph  $G(C) = \langle V, E - C \rangle$  separated from  $G$ ,  $C$  is called a graph-cut. Normally, the cost function of a graph-cut is obtained by computing the sum of the weights of the edges in  $G$ :

$$\text{cost}(\sum_{e \in C} w_e) \tag{1}$$

The minimum cut [12] among all possible graph-cuts is the optimal binary segmentation of  $G$ .

Consider an arbitrary image with a set  $P$  including all image pixels, and a set  $N$  including all unordered edges  $\{p, q\}$  of eight-neighborhood elements in  $P$ .  $P$  can be divided into three parts: "object" pixels, "background" pixels and "unknown" pixels. The goal of interactive

graph-cut method is to find the global optimal solution among all segmentations satisfying the hard constraints, which is imposed by manual. Under a graph-cut of  $C$ , let  $A(C) = (A_1(C), \dots, A_p(C), \dots, A_{\|P\|}(C))$  be a two-value vector with  $p \in P$  and the number of points  $\|P\|$ . The value of  $A_p(C)$ ,  $p \in P$  be specified by the following formula:

$$A_p(c) = \begin{cases} 1, & p \in \text{object} \\ 0, & p \in \text{background} \end{cases} \tag{2}$$

Let total energy, region energy and boundary energy [11] are defined respectively as  $E(A)$ ,  $R(A)$  and  $B(A)$ :

$$E(A) = \lambda \cdot R(A) + B(A), \tag{3}$$

where

$$R(A) = \sum_{p \in P} R_p(A_p), \tag{4}$$

$$B(A) = \sum_{\{p,q\} \in N} B_{\{p,q\}} \cdot \delta_{\{p,q\}} \tag{5}$$

and

$$\delta_{\{p,q\}} = \begin{cases} 1, & A_p \neq A_q \\ 0, & A_p = A_q \end{cases} \tag{6}$$

The parameter  $\lambda \geq 0$  in (3) reflects the significant degree of region energy term  $R(A)$  and boundary energy term  $B(A)$  in total energy term  $E(A)$ . The term  $R(A)$  reflects the cost of  $p$  assigned to "object" or "background". If  $p$  is similar to the "background", the value of  $R_p$ ("background") is very small. The term  $B(A)$  comprises the boundary energy of segmentation,  $B_{\{p,q\}}$  is large when  $p$  and  $q$  are similar each other and close to 0 when  $p$  and  $q$  are awfully different.

Optimal image segmentation is equivalent to combinatorial optimization problem:

$$\min_{c \in C} (E(A)) = \min_{c \in C} (\lambda \cdot R(A) + B(A)) \tag{7}$$

Fig. 1 illustrates the optimal binary segmentation process of a  $3 \times 3$  image. In Fig. 1 (a), the source set is  $O$  and the terminate set is  $B$ . The weight of each edge in Fig. 1 (b) is reflected by the edge's thickness. The regional energy term (4) define the costs of terminal links. The boundary energy term (5) defines the costs of neighborhood links. In Fig. 1 (c-d), these two parts corresponds to a segmentation of the image in Fig 1 (a). A minimum cut produces a binary segmentation that is optimal binary segmentation in accordance with regional energies and boundary energies that are built into the edge costs.

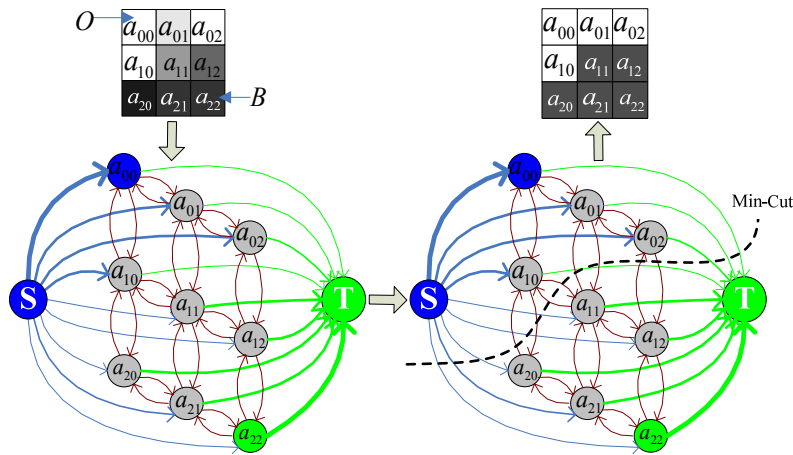


Fig. 1 A 3×3 image segmentation process of graph-cuts

III. INTERACTIVE LiDAR DATA SEGMENTATION

As the ground point can be removed by building digital terrain model (DTM), we only take the classification of building and vegetation into account in this paper.

Let  $P'$  is a set of LiDAR data, and  $A = (A_1, \dots, A_{p'}, \dots, A_{\|P'\|})$  is a cut of  $P'$ . Where  $p' \in P'$ ,  $\|P'\|$  is the sum of LiDAR point clouds and  $A_{p'}$ :

$$A_{p'} = \begin{cases} 1, & p' \in object \\ 0, & otherwise \end{cases} \quad (8)$$

A. Feature Vectors Extraction

In the classification of LiDAR data, the most widely related method is bases on feature vectors. In general, the building's surface is more regular than vegetation's. This means that the characteristic properties of building's points are probably consistent with each other, or may be have some small differences at the edge of the building. However, Trees, vegetations, etc. are not the same as building. Owing to the growth of trees and vegetations etc. is irregular, the unique properties of building's points can be collected to distinguish between buildings and no-buildings.

Assume that  $\forall p' \in P'$ , and  $M_{p'}$  denotes the set of points within  $\delta$  - neighborhood of point  $p'$ :

$$M_{p'} = \{q' | q' \in P', \|p' - q'\| < \delta\} \quad (9)$$

$\bar{p}$  is the centroid of all points in  $M_{p'}$ :

$$\bar{p} = \frac{1}{\|M_{p'}\|} \cdot \sum_{q \in M_{p'}} q \quad (10)$$

According to the above analysis, building points should have the following geometry features:

**Feature 1:** Normally, The sample points collected around a building point should be close to a plane. So in this paper, all points in  $M_{p'}$  can be seen as a plane. The

least-squares method applied to fitting the plane equation  $K$ . Then the mean square error  $\sigma^2$  calculated by means of the following formula:

$$f_1^{p'} = \sigma^2 = \frac{1}{\|M_{p'}\| - 1} \cdot \sum_{i=1}^{\|M_{p'}\|} [L(p'_i, K)]^2, \quad (11)$$

where the term  $L(p', K)$  is Euclidean distance formula to measure the distance from point  $p'$  to plane  $K$ . If the value of  $f_1^{p'}$  is close to zero, that is to say, actually, the points in  $M_{p'}$  are most likely in the fitting plane  $K$ . Namely, these points are most likely to belong to building.

**Feature 2:** As we have discussed above, LiDAR captures the surface information of the building, the normal vectors of building surface points should be consistent in  $M_{p'}$ . We can estimates the normal vectors  $\vec{n}_{p'}$  of  $p'$  applying the directional vector of  $K$ , then consider their sum:

$$f_2^{p'} = \sum_{i=1}^{\|M_{p'}\|} \text{arc}(\vec{n}_{p'}, \vec{n}_{p_i}) \quad (12)$$

Where  $\text{arc}(\vec{n}_{p'}, \vec{n}_{p_i})$  corresponds to the angle of  $\vec{n}_{p'}$  and  $\vec{n}_{p_i}$ , when they are tend to parallel, the vector of  $\text{arc}(\vec{n}_{p'}, \vec{n}_{p_i})$  is close to zero. At the same time, it indicates that the possible type of point  $p'$  should belong to the building.

**Feature 3:** Normally, LiDAR points cloud around a building point's  $\delta$  - neighborhood should be regular [14], so the Euclidean distance  $p'$  and  $\bar{p}$  of set  $M_{p'}$  is more likely to zero.

$$f_3^{p'} = |p' - \bar{p}| \quad (13)$$

**Feature 4:** The authors of [14, 15] estimates local surface properties using a statistical analysis of the neighboring points. In particular, covariance matrix analysis method is an efficient algorithm for estimating the characteristics of the building points. Firstly, the 3×3

covariance matrix  $C_{p'}$  of  $M_{p'}$  can be calculated by the following formula:

$$C_{p'} = \begin{bmatrix} p'_i - \bar{p} \\ \dots \\ p'_{|M_{p'}|} - \bar{p} \end{bmatrix}^T \cdot \begin{bmatrix} p'_i - \bar{p} \\ \dots \\ p'_{|M_{p'}|} - \bar{p} \end{bmatrix} \quad (14)$$

Where  $C_{p'}$  describes the statistical properties of the distribution of the points in the  $\delta$ -neighborhood of  $p'$  by accumulating the squared distances of these points from  $\bar{p}$ .

Secondly, the three eigenvalues  $\lambda_0, \lambda_1, \lambda_2$  of the matrix  $C_{p'}$  calculated. Assuming  $\lambda_0 \leq \lambda_1 \leq \lambda_2$ . The value of  $\lambda_0$  describes the variation along the surface normal and it is defined as:

$$f_4^{p'} = \frac{\lambda_0}{\sum_{i=0}^2 \lambda_i} \quad (15)$$

The surface variation  $f_4^{p'}$  corresponds to the distribution of points set  $M_{p'}$ . It indicates that all points lie in a plane when  $f_4^{p'} = 0$ .

Finally, a set of feature vectors will be obtained:

$$\{F^{p'} = (f_1^{p'}, f_2^{p'}, f_3^{p'}, f_4^{p'}) | p' \in P'\} \quad (16)$$

Fig. 2 shows the corresponding feature classification of LiDAR data. The left part of Fig. 2 is original LiDAR data, and the right part is feature classification results.

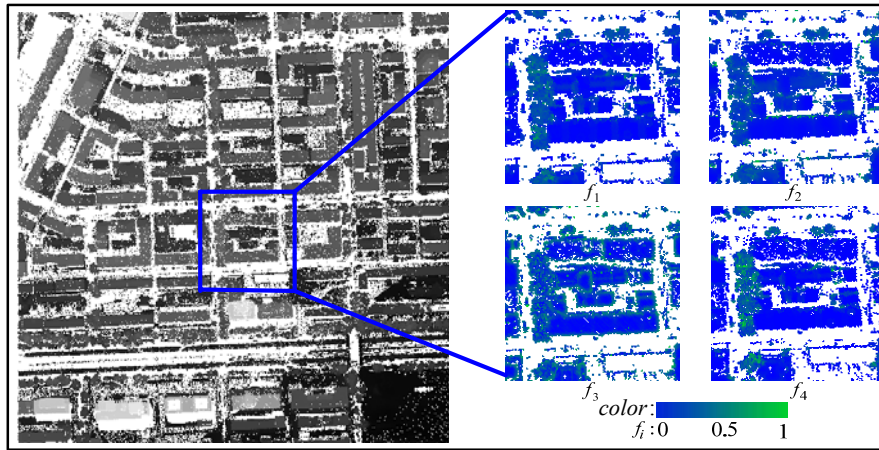


Figure 2. The distribution of features of LiDAR data

**B. Graph Construction**

Assume that  $O$  and  $B$  represent the subsets of LiDAR points data marked as "object" and "background", satisfying  $O \subset P'$ ,  $B \subset P'$  and  $O \cap B = \Phi$ . In order to segment LiDAR data using interactive graph-cut, we construct a graph  $G' = (V', E')$ .  $V'$  is node set that contains each point of  $P'$ , a source node  $S$  and a sink node  $T$ , where  $S$  and  $T$  connect all points of  $P'$ . So set  $V'$  denoted as:

$$V' = P' \cup \{S, T\}$$

Edge set  $E'$  contains two types of edges: neighborhood links and terminal links. Each point has two terminal links  $\{p', S\} \in E'$  and  $\{p', T\} \in E'$ . Each pair of neighboring points satisfying condition  $|p' - q'| < \delta$  is connected by a neighborhood link, namely  $\{p', q'\} \in E'$ . All adjacent points in  $P'$  constitute a set of edges named  $N$ . We can get a set:

$$E' = N \cup \{\{p', S\}, \{p', T\}\} \cup \dots \cup \{\{p'_{|p'|}, S\}, \{p'_{|p'|}, T\}\}$$

We can set the weight of each edge  $\{p', q'\} \in E'$  by the following formula:

$$w_{\{p', q'\}} = \begin{cases} B_{\{p', q'\}}, & \{\{p', q'\} \in N\} \\ \lambda R_{p'}(\text{"background"}), & \{p' \in P', p' \notin O \cup B, q' = S\} \\ \lambda R_{p'}(\text{"object"}), & \{p' \in P', p' \notin O \cup B, q' = T\} \\ K, & \{p' \in B, q' = T\} \text{ or } \{p' \in O, q' = S\} \\ 0, & \{p' \in B, q' = S\} \text{ or } \{p' \in O, q' = T\} \end{cases} \quad (17)$$

where  $K = 1 + \max(\sum_{p' \in P'} \sum_{q': \{p', q'\} \in N} B_{\{p', q'\}})$

In [11], the author has proven the existence of the min-cut  $C_{\min}$  on  $G'$ . At the same time, the  $C_{\min}$  corresponding to  $A(C_{\min})$  satisfying the following hard constraints:

$$A_{q'} = \begin{cases} \text{"object"}, & \forall q' \in O \\ \text{"background"}, & \forall q' \in B \end{cases} \quad (18)$$

**C. Energy Function**

What needs to be pointed out is that the calculation method of energy function is not unique. Generally, function meeting the following conditions can be used as energy function:

- 1) If the point  $p'$  is similar to the point in user-specified background set, the value of  $R_{p'}(\text{"background"})$  is small. If the point  $p'$  is similar to the point in user-specified object set, the value of

$R_p$  ("object") is small.

2) If the features of any two adjacent points are similar, the value of  $B_{\{p,q\}}$  is big. Otherwise small.

In this paper, the energy function computed by the feature vectors, which identified in section 3.1. Gaussian mixture model (GMM) method be used to determine the probability density function of  $O$  and  $B$  respectively. Then the conditional probability of LiDAR points estimated by  $P(p'|O)$ ,  $P(p'|B)$ , where  $p' \in P'$ . According to the MAP-MRF formula mentioned in [16], we set:

$$R_{p'}(\text{"object"}) = -\ln P(p'|O) \quad (19)$$

$$R_{p'}(\text{"background"}) = -\ln P(p'|B) \quad (20)$$

In addition, the boundary energy function can be simplified calculated as follows [11]:

$$B_{\{p',q'\}} = e^{-\|F^{p'} - F^{q'}\|} \quad (21)$$

#### D. Parameter Estimation

In the formula (3), Parameter  $\lambda$  reflects the relation of  $B$  and  $R$ , affecting the value of  $E$ . In the segmentation process, different  $\lambda$  values lead to different segmentation result. It requires an estimate of  $\lambda$  optimal value  $\hat{\lambda}_{opt}$ . In this article, sample-fitting method proposed to estimates optimal value  $\hat{\lambda}_{opt}$ .

Assume that  $D$  is a subset of the LiDAR data, namely  $D \subseteq P$ . The classification of  $D$  has been labeled by manual with  $O_D$  and  $B_D$ , satisfying  $O_D \subset D$ ,  $B_D \subset D$ . According to a certain interval  $\zeta$ , a sequence of values can be obtained:

$$Q = \{\lambda_0 = 0, \dots, \lambda_i = i \cdot \zeta, \dots\}$$

For each value  $\lambda_i \in Q$ , A segmentation result of  $D$  can be computed by using the proposed segmentation method in this paper. From the segmentation result, we can get an "object" set  $D_{\lambda_i} \subset D$ . The accuracy of segmentation calculated by:

$$R_{\lambda_i} = \frac{\|D_{\lambda_i}\|}{\|D\|} \quad (22)$$

Where  $\lambda_i \in Q$ , and  $\|D\|$ ,  $\|D_{\lambda_i}\|$  denotes the number of  $D$ ,  $D_{\lambda_i}$  respectively.

A subset  $Q_1$  from  $Q$  be obtained according to a certain way of sampling, :

$$Q_1 = \{\lambda_{i_1}, \lambda_{i_2}, \dots, \lambda_{i_{n-1}}, \lambda_{i_n}\}$$

We can extend the set  $Q_1 \rightarrow Q_2$  :

$$Q_2 = \{(\lambda_{i_1}, \hat{R}_{i_1}), (\lambda_{i_2}, \hat{R}_{i_2}), \dots, (\lambda_{i_{n-1}}, \hat{R}_{i_{n-1}}), (\lambda_{i_n}, \hat{R}_{i_n})\}$$

The least squares method is used to fitting  $Q_2$  :

$$\hat{R} = S(\lambda) \quad (23)$$

The maximum peak of fitting curve  $S$  is  $\hat{R}_{max}$ . The corresponding  $\lambda$  value of  $\hat{R}_{max}$  is the estimates of  $\hat{\lambda}_{opt}$ . Approximate estimation errors obtained using the following formula:

$$\varepsilon \approx |1 - \hat{R}_{max}| \quad (24)$$

#### IV. EXPERIMENTS AND ANALYSIS

Experiments are performed on an Intel (R) Core (TM) Duo E7200 computer running at 2.53 GHz. To test the validity of the proposed method, experimental LiDAR data set with multiple roof shapes and trees area is selected for the experiment. Data set is a small part of XXX city in China. The density of points of LiDAR data set is approximately 2.25 points/m<sup>2</sup>. The total number of points in test data set is 423, 438 points. The original LiDAR data is shown in Fig. 3:

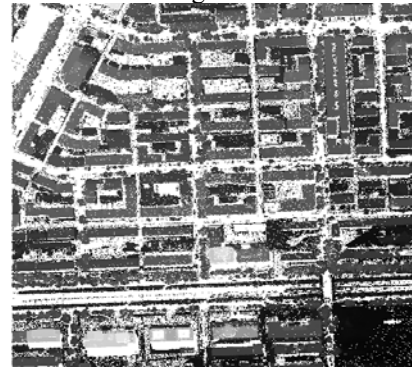


Fig 3 Original LiDAR data

In order to define and calculate the accuracy of segmentation algorithm in this paper, we set classification of all LiDAR points manually:

$$A_{manul} = (A_{manul,1}, \dots, A_{manul,p'}, \dots, A_{manul,\|P'\|})$$

The result of classification is shown in Fig. 4:

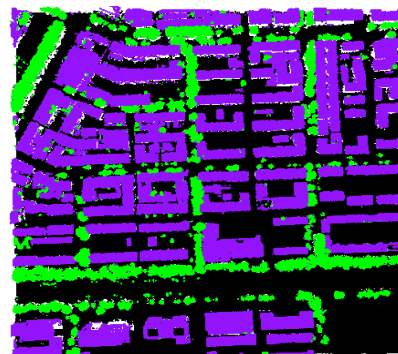


Fig. 4 Classification result by manual

In Fig. 4, the green part represents trees and vegetation, pink part represents the building and black part represents land.

The final segmentation results by our algorithm are denoted as:

$$A_{graphcut} = (A_{graphcut,1}, \dots, A_{graphcut,p'}, \dots, A_{graphcut,\|P'\|})$$

So the segmentation accuracy of  $P'$  can be divided in accordance with the following formula:

$$R = \frac{\sum_{i=0}^{\|P'\|} (1 - |A_{graphcut,i} - A_{manul,i}|) A_{manul,i}}{\|P'\|} \quad (25)$$

**Experiment 1. Parameter  $\lambda$  estimation experiment**

In the LiDAR test data, a region is extracted:

$$D = \{p'(x, y, z) | 0 \leq x, y \leq 100\}$$

The manual classification result of points for  $D$  is shown in Fig. 5:

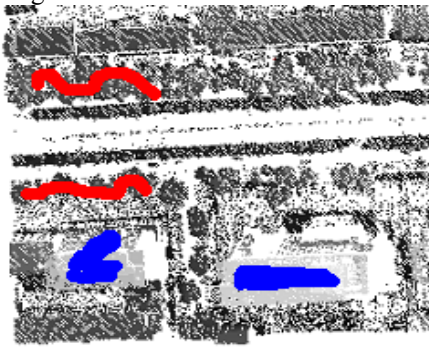


Fig. 5 Sub-set D, "object" and "background" points

Where the blue part is a "object" region and the red part is a "background" region.

The interval of  $[0, 1]$  is divided into 50 equal portions. Each split point can be denoted as  $\lambda_i = 0.02 * i, 0 \leq i \leq 50$ . So we can get  $Q_2$  based on the above method in section 3.4. Least-squares fitting method can be used fitting a curve of second degree shown in Fig. 6:

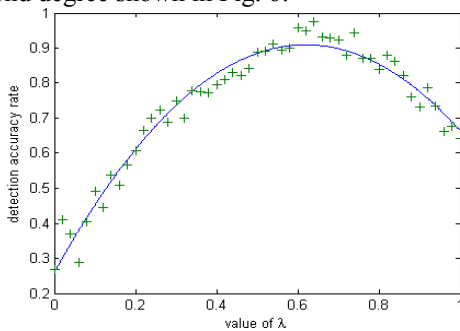


Fig. 6 Least-squares method fitting  $Q_2$  result

Experiment shows that result is the best one when  $\hat{\lambda}_{opt} \approx 0.6630$ . Therefore  $\lambda$  is set to 0.6630 in the following experiments.

**Experiment 2. Segmentation experiment**

The segmentation accuracy of LiDAR data based on interactive graph-cut theory is shown in Table I.

TABLE I.  
SEGMENTATION STATISTICS

Manual times	Number of "object" points	Number of "background" points	Segmentation accuracy	Execution time (min)
1	694	926	64.6%	3.24
2	314	517	78.3%	3.59
3	375	322	84.1%	4.58
4	219	384	93.4%	4.93

5	176	195	95.8%	5.30
---	-----	-----	-------	------

As can be seen from the table 1, with the number of points by manual increasing, the segmentation accuracy is increasing quickly. Adding a small number of "object" points and "background" point, the accuracy rises to 90% easily. When the segmentation accuracy rate is up to 95%, the total number of "object" points only need 1, 778 points, and "object" points only need 2, 344 points. Result is shown in Fig.7:



Fig. 7 Segmentation result

In Fig. 7, some points marked as red color are classification wrong points by our method, which mainly concentrated in the edges of buildings, trees or vegetation. Therefore building extraction and modeling in the future is not affected.

V. CONCLUSIONS

In this paper, the extraction of buildings from LiDAR data based on the theory of interactive graph-cut is proposed. Firstly, we apply four-dimensional feature vectors to compute the region energy and boundary energy of each LiDAR point. Secondly, the Parameter  $\lambda$  is estimated by a new sample-fitting method. Thirdly, we apply interactive graph-cut method to obtain the optimal two-value segmentation of all LiDAR points. After all these steps above, most points of buildings are obtained. By the experiment, our method can extracts building area from LiDAR data accurately. This paper's algorithm has a strong adaptability in the situation of buildings and trees connected to each other.

ACKNOWLEDGEMENT

This work is supported by the grants from the National Natural Science Foundation of China [Grant No. 60873147] and Science and Technology Development Program of Jilin Province [Grant No 20060527].

REFERENCES

[1] Aloysius Wehr, Uwe Lohr, Airborne laser scanning-An introduction and overview [J], ISPRS Journal of Photogrammetry & Remote Sensing, 1999, 54 (2-3): 68-82.  
 [2] Jung J. Crawford M. M., Extraction of Features From LIDAR Waveform Data for Characterizing Forest Structure [J], IEEE Geoscience and Remote Sensing Letters, 2011, 1 (99): 1-5.

- [3] Gunho Sohn, Ian J., Dowman. Dowman, A model-based approach for reconstructing a terrain surface from airborne LIDAR data [J], *Photogrammetric Record*, 2008, 23 (122): 170-193.
- [4] K. Zhang, J. Yan, and S. Chen, Automatic construction of building footprints from airborne LIDAR data [J], *IEEE Trans, Geoscience and Remote Sensing*, 2006, 44 (9): 2523-2533.
- [5] Zhi Wang, Li-Xin Wu, Automated extraction of building geometric features from raw LiDAR data[C] //2009 IEEE International Geoscience and Remote Sensing Symposium, IGARSS 2009 (IGARSS'2009), Cape Town, South Africa: Institute of Electrical and Electronics Engineers Inc, 2009: 436-439.
- [6] Yun-Woong Choi, Young-Woon Jang, Hyo-Jong Lee, Gi-Sung Cho, Three-Dimensional LiDAR Data Classifying to Extract Road Point in Urban Area [J]. *IEEE Geoscience and Remote Sensing Letters*, 2008, 5 (4): 725-729.
- [7] Weidner, U. Foestner, W. Towards automatic building extraction from high resolution digital elevation models [J]. *ISPRS Journal of Photogrammetry and Remote Sensing*, 1995, 50 (4): 38-49.
- [8] Zhu Ling-Li, Hyypä Juha, Kukko Antero, Kaartinen Harri, Chen Ruizhi. On the quality of object classification and automated building modeling based on lasers scanning data[J]. *Remote Sensing*, 2011, 3 (7): 1406-1426.
- [9] Shu Weng, Gang Zhao, Bin He. Rapid reconstruction of 3D building models from aerial images and LiDAR data[C]//2010 3rd International Conference on Advanced Computer Theory and Engineering (ICACTE'2010). Chengdu, China: IEEE Computer Society, 2010, 2195-2198.
- [10] Mao Jian-hua, Liu Xue-feng, Zeng Qi-hong. Building extraction by fusion of LIDAR data and aerial images[C]// 2009 Joint Urban Remote Sensing Event, Shanghai, China: IEEE Computer Society, 2009.
- [11] Boykov Y. Y. Jolly M.-P. Interactive Graph Cuts for Optimal Boundary & Region Segmentation of Objects in N-D Images[C]//Proceedings of the IEEE International Conference on Computer Vision, Vancouver, BC, United States: Institute of Electrical and Electronics Engineers Inc. 2001: 105-112.
- [12] C. Rother, A. Blake, V. Kolmogorov, Grabcut—interactive foreground extraction using iterated graph cuts[C]// Proceedings of ACM Transactions on Graphics (SIGGRAPH). New York, NY, USA: Penn Plaza, Suite 701 New York NY USA, 2004, 23 (3): 307~312.
- [13] Wu Zhenyu, Leahy Richard, An Optimal Graph Theoretic Approach to Data Clustering: Theory and Its Application to Image Segmentation [J], *IEEE Transactions on Pattern Analysis and Machine Intelligence*, 1993, 15 (11): 1101-1113.
- [14] Zhou Qian-Yi, Neumann Ulrich. Fast and Extensible Building Modeling from Airborne LiDAR Data[C]//GIS: Proceedings of the ACM International Symposium on Advances in Geographic Information Systems (ACM GIS'2008). New York, NY, USA: Penn Plaza, Suite 701 New York NY USA, 2008: 1-8.
- [15] PAULY M. Point primitives for interactive modeling and processing of 3D geometry [M]. Switzerland: ETH Zurich, pp: 13-18, 2003.
- [16] Boykov Yuri, Veksler Olga, Zabih Ramin. Markov random fields with efficient approximations[C]// Proceedings of the IEEE Computer Society Conference on Computer Vision and Pattern Recognition, Los Alamitos, CA, United States: IEEE Comp Soc, 1998: 648-655.

**Wen-Hui Li** was born in 1961. He is a Professor and doctor supervisor in College of Computer Science and Technology, Jilin University, Changchun, P.R. China. His major research interests include computer vision, image processing, pattern recognition, graphics, virtual reality, CAD and geometric constraint.

**Hong-Yin Ni** was born in 1984. He received his M.S. degree majoring in Technology of Computer Application in 2009 from Computer Science and Technology, Jilin University, P. R. China. He is studying for his Ph.D. in the College of Computer Science and Technology, Jilin University. His research interests include computer image processing, pattern recognition and virtual reality technology.

**Hui-ying Li** is a Lecturer of Jilin University, China. She received the B.E., M.S. and PhD degree in Computer Science and Technology from Jilin University, China, in 2001, 2004 and 2008 respectively. She was a visiting scholar to the Department of Electrical and Computer Engineering in University of Hannover from 2007 to 2009. Her research interests include computer algorithms and simulation, image processing and 3D modeling.

**Ying Wang** was born in 1983. She received her M.S. degree majoring in software engineering in 2008 from College of Software, Jilin University, P. R. China. She is now pursuing her Ph.D. at Image Processing and Virtual Reality Technology Lab in the College of Computer Science and Technology, Jilin University. Her research interests include face recognition, fire/smoke detection, pedestrian detection and object tracking.

**Bo Fu** was born in 1983. Since 2009, He has been working on the PhD degree in College of Computer Science and Technology, Jilin University, Changchun, P. R. China. His research interests include computer image processing, image denoising, and pattern recognition and anomaly intrusion within the video region.

**Yi-feng Lin** was born in 1982. He received the B.Sc. in 2005 and M.S. 2007 in College of Computer Science and Technology, Jilin University, Changchun, P. R. China. He has been working on the PhD degree in this college since 2007. His research interests include computer vision, image processing, pattern recognition, machine learning and 3D virtual engine. He especially has been researching in detection of human face and human body, supervised and semi-supervised learning, image classification and image retrieval. His papers are presented in several international journals and conferences.

**Pei-xun Liu** was born in 1986. Since 2011, He has been working on the PhD degree in College of Computer Science and Technology, Jilin University, Changchun, P. R. China. His research interests include computer vision, image processing and pattern recognition.